

# Spatio-temporal variability of snow water equivalent over the Vestre Broggerbreen and Feiringbreen glaciers, Ny-Ålesund, Svalbard

LAVKUSH PATEL\* , PARMANAND SHARMA and MELOTH THAMBAN

National Centre for Polar and Ocean Research, Vasco-Da-Gama, Goa 403 804, India.

\*Corresponding author. e-mail: lavkushpatel@ncaor.gov.in

MS received 14 November 2018; revised 6 May 2019; accepted 8 May 2019; published online 5 July 2019

Snow water equivalent (SWE) is important for understanding the hydrological significance of glaciers. In this study, the spatial and temporal variability in SWE and its impact over the Vestre Broggerbreen and Feiringbreen glaciers around Ny-Ålesund in Svalbard (high Arctic) were investigated in the early snow season for the period 2012–2017. The physical properties like depth and density were measured directly in the field and spatial characteristics curvature, slope and aspect were extracted from the digital elevation model. The Vestre Broggerbreen (4.1 km<sup>2</sup>) is a NE flowing glacier, situated around 3 km SW to Ny-Ålesund village while the Feiringbreen (7.5 km<sup>2</sup>) is a SW flowing glacier, situated around 14 km NE across the Kongsfjorden. The SWE for the studied period (2012–2017) varied from 141 to 1188 mm. The significant ( $R^2 = 0.97$ ) correlation indicated a possible control of snow depth over SWE compared to altitude ( $R^2 = 0.65$ ) and other spatial characteristics. The glaciers have experienced negative balance and lost a significant amount of ice ( $\sim 4$  m.w.e.) since 2012. The observations suggest that the increased liquid precipitation and temperature in the early snow season have reduced SWE over both these valley glaciers. The reduced SWE has also contributed to decreases in the mass balance of these glaciers.

**Keywords.** Mass balance; snow water equivalent; Vestre Broggerbreen; Feiringbreen; Svalbard.

## 1. Introduction

Snow is an important component of the cryosphere, which affects the glacier surface mass balance (SMB), local climate, permafrost regime, large-scale atmosphere circulation and annual carbon budget (Bruland and Sand 2001; Boike *et al.* 2003; Hallinger *et al.* 2010; Callaghan *et al.* 2011; Eckertorfer and Christiansen 2011; Derksen and Brown 2012). The seasonal snowpack has a great impact on atmospheric circulation by modifying the land surface albedo and temperature as well as through changes in the land-surface energy budget.

The snowpack response to climate change may be altered by the length of the snow season, and fluctuations in the amount of snow accumulated throughout the winter/year. Snow water equivalent (SWE) characterises the hydrological significance of the snow cover. Therefore, monitoring of temporal and spatial variability of the SWE is significant for predicting the glacier behaviours including water budget.

SWE is defined as the total volume of water present in a snowpack if the entire snowpack is melted (Egli *et al.* 2009). The SWE is an important parameter for snow hydrology, snow climatology

and avalanche formations (Egli *et al.* 2009; Rice *et al.* 2011; López-Moreno *et al.* 2016). The SWE can be estimated by snow depth ( $h_s$ ) and bulk density ( $\rho$ ) (Jonas *et al.* 2009), automatic methods and empirical models (Skaugen 2007; Egli *et al.* 2009; Clark *et al.* 2011; Clow *et al.* 2012; Bavera *et al.* 2014; Cornwell *et al.* 2016), ground penetrating radar (Pälli *et al.* 2002; Godio and Rege 2016; Holbrook *et al.* 2016) and remote sensing techniques (Foster *et al.* 2005). The SWE was measured at several regions for the characterisations of snow cover and also for the validation of several models (Liston and Sturm 2002; Bocchiola and Rosso 2007; Sturm *et al.* 2010; Rice *et al.* 2011; López-Moreno *et al.* 2013, 2016; Cornwell *et al.* 2016).

Snow dominates the entire Svalbard landscape including ice-caps and glaciers for 8–10 months of the year (López-Moreno *et al.* 2016). Snow accumulation over the Svalbard region is significantly governed by the precipitation intensity, topography and wind (Van Pelt *et al.* 2016). Surface topography (slope, aspect and surrounding higher mountains) has a profound influence on the surface energy balance over the glaciers and significantly controls the state of the snowpack (Arnold *et al.* 2006; Kerner *et al.* 2013). The surface energy balance is crucial to understand the link between atmospheric forcings and snow and ice characteristics on a glacier. Long wave radiation and turbulent fluxes are the dominant sources of energy balance during winter (October–April). The energy fluxes strongly affect the physical properties of the glacier surface and significantly regulate the SWE.

The Svalbard archipelago lies at the northern extremity of the warm North Atlantic current and is sensitive to climate shifts (Hagen *et al.* 2003). The glaciers of Svalbard archipelago have a significant influence on water circulation within the surrounding sea and fjords. Recently, increasing variability in temperature and precipitation related to ‘Arctic amplification’ has been found to significantly impact on the snow cover of the Svalbard region (Serreze *et al.* 2009; Van Pelt *et al.* 2016). In recent years, studies have been carried out in Svalbard to better understand the spatial and seasonal pattern of the snow cover and its impact on variability (Bruland *et al.* 2004; Möller *et al.* 2011; Van Pelt *et al.* 2016). It was reported that the SWE is largely controlled by winter accumulation and the increased warming in this region has shifted the equilibrium line altitude

(ELA) in glaciers around the Ny-Ålesund (Van Pelt *et al.* 2016). The winter accumulation is linked to the precipitation pattern and the winter is also more sensitive to climate change than the summer (López-Moreno *et al.* 2016). The atmospheric circulation pattern and the inhomogeneous precipitation over Svalbard have a substantial impact over the Ny-Ålesund glaciers and their water budget.

Several studies are available for the glaciers like Austre Broggerbreen, Midtre Lovenbreen, Kongsvegen, Kronebreen, Kongsbreen, etc. around the Ny-Ålesund region, but very few are reported for the Vestre Broggerbreen and Feiringbreen glaciers. In this study, the variability in the snow accumulation pattern over the Vestre Broggerbreen and Feiringbreen glaciers were measured during the early snow season (October–March) for the years 2012–2017. The spatial pattern and major factors for SWE influence were analysed, and their impacts on glaciers were also observed. The study will be helpful for the validation of the available hydrological models and snow models.

## 2. Data and methods

### 2.1 Study area

The Vestre Broggerbreen and Feiringbreen, two valley glaciers around Ny-Ålesund (78°56′N; 11°53′E), Svalbard Archipelago have been selected for the present study. The Vestre Broggerbreen (78°53′–78°56′N; 11°36′–11°48′E), a NE flowing valley glacier, is situated 3 km SW Ny-Ålesund, while Feiringbreen (79°0′–79°05′N; 12°10′–12°40′E) is a SW flowing valley glacier, situated 14 km NE of Ny-Ålesund, across the Kongsfjorden (figure 1). The Vestre Broggerbreen glacier is ~4 km long and covers an area of ~4.2 km<sup>2</sup> with altitude varying from 90 to 720 m.a.s.l. (figure 2a). The length and area of the Feiringbreen glacier are ~5.4 km and ~7.5 km<sup>2</sup>, respectively, with the relief ranging from 210 to 970 m.a.s.l. (figure 2b). The annual mean temperature at Ny-Ålesund during 2012–2017 was –4.2°C. The mean temperature from October to February was –9.2°C while it was –1.4°C from March to June. The average annual precipitation was 415.5 mm, with 198.7 mm from October to February and 81.8 mm from March to June (López-Moreno *et al.* 2016).

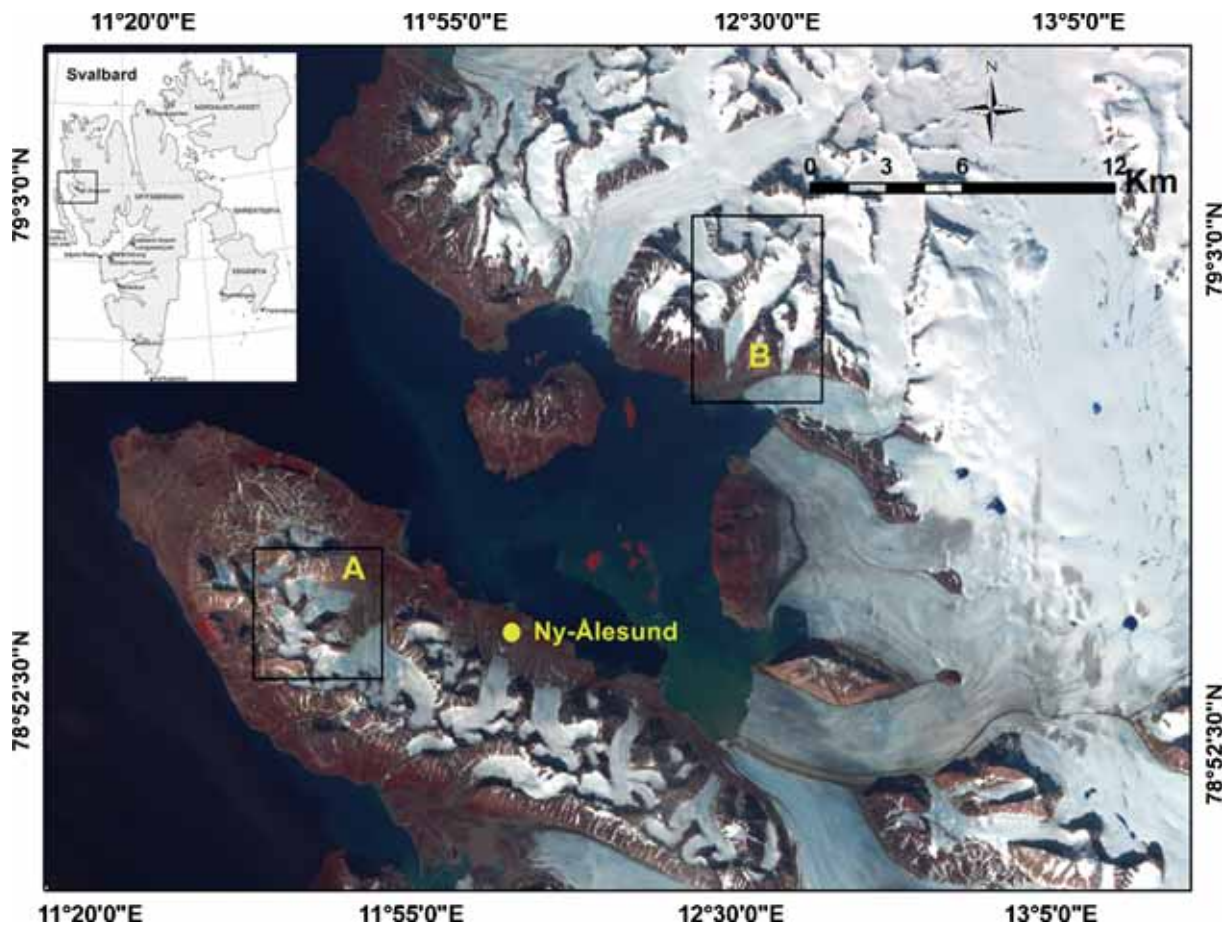


Figure 1. Location of the selected glaciers in Svalbard.

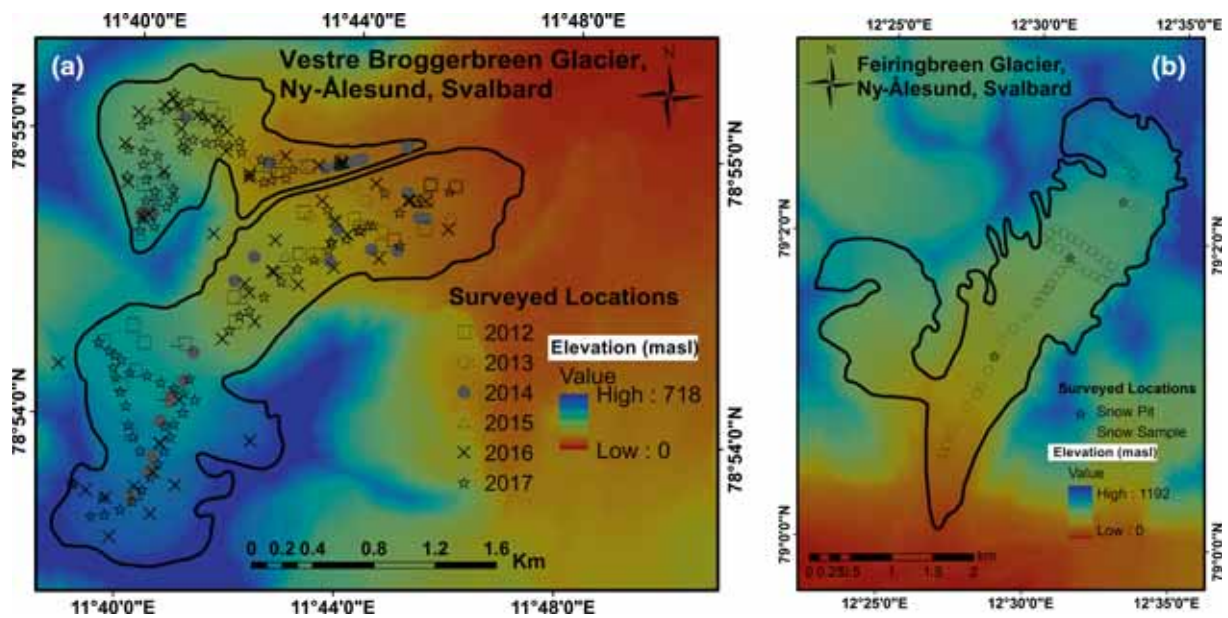


Figure 2. Surveyed locations of (a) Vestre Broggerbreen (2012) and (b) Feiringbreen (2016).

## 2.2 Snow observations

Observations were carried out to measure the snow accumulation pattern and estimate the temporal and spatial SWE variability across the glaciers for the period 2012–2017. The SWE is the product of snow depth and snow density (Jonas *et al.* 2009; Sturm *et al.* 2010). The depth and density of snow were measured by digging snow pits, snow probing and retrieval of snow cores in a flat and open site over Vestre Broggerbreen in April 2012–2017 (figure 2a). The Feiringbreen glacier was surveyed and studied only during 2016 due to logistic constraints (figure 2b). The details of snow observations for each year are given in table 1. Additionally, a snow core was used for the density measurement for the years 2015 and 2016, while a snow fork (Model LK 2010 by Toikka Oy) was used for snow density observations in 2017. The locations of snow pits and cores were selected in such a way that they are undisturbed and are along with the central flow of the glacier. We have repeated the snow observations closely by place for the following year and took the observation from all methods (snow core, pit and snow fork) for comparison in the year 2017. Each snow pit was made at the north-facing walls to avoid disturbance by insolation during sampling and excavated down to the ice layer. This ice layer represents the previous summer surface. The snow samples were collected in a measuring cylinder of a known weight and weighed in a precise weighing balance. The total volume was divided by the weight of the collected snow. A Kovacs Mark II coring system was used to take snow cores for depth and density measurements. While taking the cores, it was taken care that no snow was lost. A tube was inserted into the base of the snowpack, rotated slightly to extract a small ice plug, the snow depth was noted and the snow core was removed. We measured 11 cores in April 2015 and 5 cores in 2016 along with the central flow of the glacier at different altitudes. Furthermore, we compared the density of the snowpack collected from the pit and the core from the same location. It was observed that the densities collected by the cores are slightly higher than the density measured from the pits. However, the average density of the snowpack was well within the acceptable range (<10%). We also used a snow fork to measure the density of the snowpack over the Vestre Broggerbreen glacier for the year 2017. The snow fork measures the resonant frequency (500–900 MHz), attenuation and 3 dB bandwidth

Table 1. Snow observations and snow characteristics in the Vestre Broggerbreen and Feiringbreen glaciers of Ny-Ålesund, Svalbard.

Year	No. of snow observations			Snow characteristics			Glacier
	Snow pit	Snow core	Snow depth (snow probe)	Average snow depth (cm)	Average snow density (g/cm <sup>3</sup> )	Average SWE (mm)	
2012	9		36	108.2 ± 58	0.41 ± 0.01	441.2 ± 238.6	Vestre Broggerbreen
2013	4		23	77.5 ± 27.3	0.37 ± 0.03	288.7 ± 106.2	Vestre Broggerbreen
2014	9		25	181.6 ± 43.3	0.4 ± 0.03	697.9 ± 185.9	Vestre Broggerbreen
2015	1	11		136.4 ± 35.6	0.4 ± 0.02	603.4 ± 162.6	Vestre Broggerbreen
2016	6 (3)	4 (1)	46 (49)	100.3 ± 49.1 (133.6 ± 56.5)	0.4 ± 0.1 (0.28 ± 0.03)	376.8 ± 172.3 (381.9 ± 187)	Vestre Broggerbreen (Feiringbreen)
2017	9		96	117 ± 42.8	0.36 ± 0.03	408.8 ± 152.1	Vestre Broggerbreen

to calculate the snow dielectric constant ( $\epsilon'$ : 1–2.9 and 0–0.15), liquid water content (0–10%) and snow density (0–0.6 g/cm<sup>3</sup>) by using the semi-empirical equations (Sihvola and Tiuri 1986). We measured the snow properties in three rows into the wall of the snow pit by pushing at vertical intervals of 10 and 20 cm horizontal intervals. The snow depth was measured by using a snow probe. Snow probe provides an unambiguous measurement point, requiring no interpretation, with an uncertainty of a few centimetres. The uncertainty in the snow probe data was estimated by the snow depth data obtained through the snow pits.

The SWE was estimated by the multiplication of the snow depth ( $h_s$ ) and snow density ( $\rho$ ). For determining the SWE, we use the average density of the same altitude zone, where depth was measured in cm and density in g/cm<sup>3</sup>, the SWE was denoted as mm. The meteorological data were obtained from the Norwegian Meteorological Service (Metno, <http://eklima.met.no/>) for the period 2011–2017 for a monthly pattern of the precipitation, temperature, wind speed and wind direction. The uncertainty in snow density estimation obtained from the core and pits with snow fork was also determined by a comparative test. The results showed that the snow density obtained from the core was relatively higher by 5–10% compared to density obtained from snow fork. The results of the comparative analysis of the snow fork and snow pit showed very less (<2%) difference.

### 2.3 Spatial analysis

The spatial characteristics (curvature, aspect and slope) of the glaciers were extracted from the digital elevation model (Norwegian Polar Institute, version: September 2017) using the ArcGIS spatial analyst module. A comparative spatial analysis between curvature, aspect and the slope was also carried out for analysing the impact of spatial characteristics on the distribution of snow density, snow depth and SWE. The spatial characteristics

were classified into defined intervals and distribution of snow density, and snow depth and SWE were compared. Curvature was classified into two categories (convex (<0) and concave (>0)), aspect was classified into four categories (0–90°, 90–180°, 180–270° and 270–359°), and slope was classified into five classes (0–5°, 5–10°, 10–15°, 15–20° and >20°). Statistical analysis was carried out with the variables snow density, snow depth, SWE, aspect, curvature, slope and elevation.

### 2.4 Mass balance

Glacier mass balance is the quantitative expression of glacier volumetric changes through time and defined as the sum of all accumulation (A) and ablation (B) processes (Cogley *et al.* 2011). We have used the direct glaciological method (Paterson 1994; Wagnon and others 2007; Zemp *et al.* 2013) to calculate the net and specific mass balance. In the ablation area, the specific mass balance has been determined based on stakes installed on the glacier down to 10–12 m deep using a Heucke steam drill system. Ice density was taken as constant at 0.900 g/cm<sup>3</sup>; however, when snow was present, the density was measured systematically by using various methods including snow fork. More than 30 ablation stakes were installed over the glacier between 50 and 400 m.a.s.l. in Vestre Broggerbreen along the central flow line including other representative locations. Accumulation measurements have been carried out each year by using a snow probe, snow core and pits in the accumulation zone. The overall specific balance,  $b_n$ , was calculated according to Paterson (1994):

$$b_n = \Sigma b_i \Delta S_i, \tag{1}$$

where  $b_i$  is the specific balance of the altitudinal range,  $i$ , of the map area  $S_i$  and  $S$  is the total glacier map area ( $S = \Sigma \Delta S_i$ ). For each altitudinal range,  $b_i$  was obtained from the corresponding stake readings or net ablation/accumulation measurements. The hypsography of the glacier was derived from

Table 2. Descriptive statistics of snow depth, snow density and spatial variables aspect, curvature, slope and altitude.

	<i>N</i>	Mean	SD	Minimum	Median	Maximum
Snow density	276	0.38	0.04	0.28	0.39	0.46
Snow depth	276	118.04	54.65	16.00	110.67	278.3
Aspect	276	102	106	0	70	359
Curvature	276	0.03	0.19	−0.83	0.02	1.2
Slope	276	6.1	3.78	0.98	5.41	36.4
Altitude	276	242.9	105.5	82.7	221.9	492

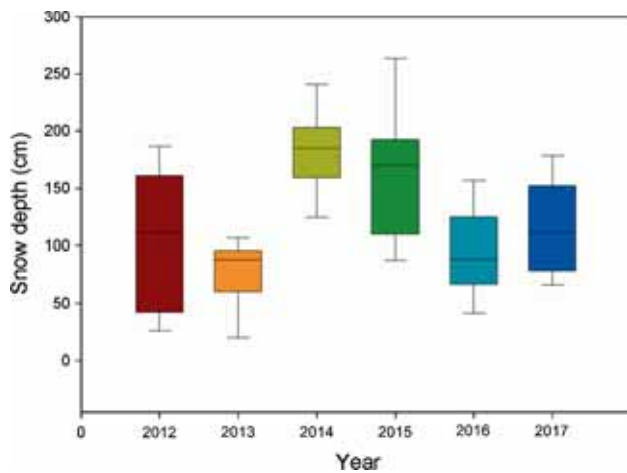


Figure 3. Snow depth pattern over the Vestre Broggerbreen glacier.

the boundary extracted from the Landsat 8 OLI image and DEM (Norwegian Polar Institute, version: September 2017).

### 3. Results

#### 3.1 Snow depth variability over the glaciers

Snow accumulation is a key element of glacier mass balance and also has great importance for the glacier state and the processes occurring on the surface as well as within the glaciers (Grabiec *et al.* 2011). Average snow depth of both the glaciers for the period 2012–2017 was  $118 \pm 55$  cm, which varied from 16 to 278 cm (tables 1 and 2). The snow depth data for the period 2012–2017 of the Vestre Broggerbreen glacier was analysed and is depicted in figure 3. In the Vestre Broggerbreen, the minimum snow depth for the years 2012–2017 varied from 16 to 76 cm while the maximum varied from 118 to 310 cm (figure 3). The snow depth gradient over the Vestre Broggerbreen varied from 16.5 to 43 cm/100 m and the lowest was observed for the year 2013, while the highest was observed for the year 2016. The highest mean snow depth ( $181.6 \pm 43.2$  cm) was in the year 2014 while the lowest ( $77.5 \pm 27$  cm) was observed in the year 2013. However, for the Feiringbreen glacier, the average snow depth was  $133.7 \pm 56.6$  cm ranging from 22 to 235 cm with a gradient of 28.3 cm/100 m (figure 4a).

The snowpack thickness over the ablation and accumulation zones was also measured separately. The ablation and accumulation zones were separated by the ELA, obtained from the mass balance data of these glaciers. In the Vestre Broggerbreen glacier, the average snow thickness was  $98.7 \pm 55$ ,

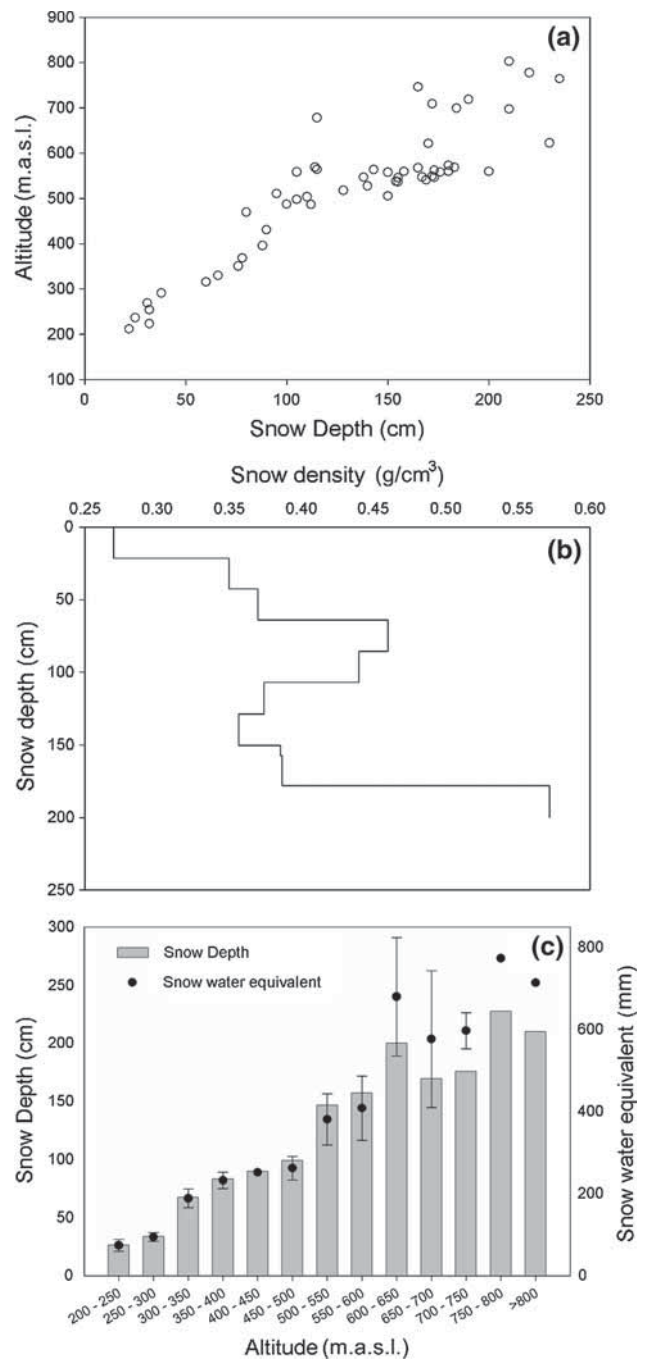


Figure 4. Snow cover characteristics (a) Snow depth, (b) snow density, and (c) snow water equivalent, over the Feiringbreen glacier for the year 2016.

$74.2 \pm 28$ ,  $165.3 \pm 37$ ,  $131.5 \pm 30$ ,  $84 \pm 31$  and  $113 \pm 42$  cm each year for the period 2012–2017 over the ablation zone, respectively. However, over the accumulation zone, the snow thickness was  $179 \pm 18$ ,  $96 \pm 5.5$ ,  $211.4 \pm 40$ ,  $200.3 \pm 44$ ,  $175.4 \pm 47$  and  $165 \pm 16$  cm, respectively, during 2012–2017. In the Feiringbreen glacier, the average snow depth during 2016 was  $191 \pm 35$  cm for the higher zone ( $>600$  m.a.s.l.),  $151.8 \pm 27$  cm for the middle zone

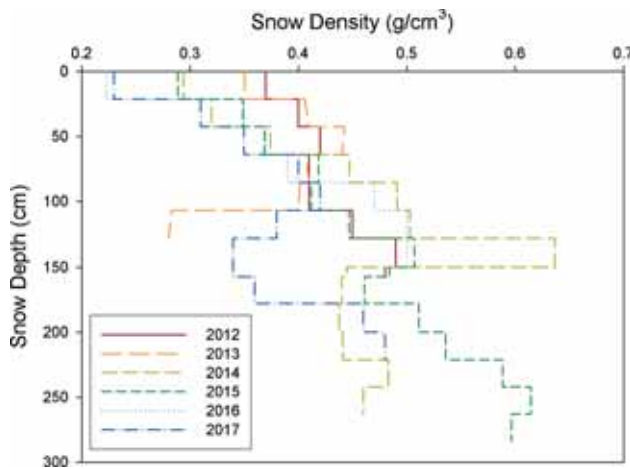


Figure 5. Bulk snow density and stratigraphy pattern over the Vestre Broggerbeen glacier during 2012–2017.

(400–600 m.a.s.l.) and  $139 \pm 67$  cm for the lower zone (<400 m.a.s.l.).

### 3.2 Snowpack density across the glaciers

Precipitation, strong winds and winter thaws are factors which mostly influence the formation of a snowpack. The observed average snow density for the period 2012–2017 was  $0.38 \pm 0.04$  g/cm<sup>3</sup>, with a minimum of  $0.28$  g/cm<sup>3</sup> and a maximum  $0.46$  g/cm<sup>3</sup> (tables 1 and 2). Figure 5 reveals the characteristics of the snowpack (average density and stratigraphic pattern) of years from 2012 to 2017 over Vestre Broggerbeen. The average bulk density for the years 2012–2017 were  $0.41 \pm 0.01$ ,  $0.37 \pm 0.03$ ,  $0.39 \pm 0.05$ ,  $0.44 \pm 0.03$ ,  $0.37 \pm 0.06$  and  $0.35 \pm 0.03$  g/cm<sup>3</sup>, respectively. The Vestre Broggerbeen has shown average snow density of  $0.39 \pm 0.05$  g/cm<sup>3</sup> and the Feiringbeen glacier  $0.34 \pm 0.09$  g/cm<sup>3</sup> (figure 4b). The snowpack density of both the glaciers revealed a positive correlation with depth and showed a higher density with increasing snow depth from the surface to the bottom. There was no significant difference observed in the density of snowpack over the ablation and accumulation zone of both the glaciers. In the Vestre Broggerbeen glacier, the average bulk density over the ablation zone during 2012–2017 was  $0.37 \pm 0.03$  to  $0.43 \pm 0.03$  g/cm<sup>3</sup> and over the accumulation zone was  $0.34 \pm 0.01$  g/cm<sup>3</sup>, respectively.

### 3.3 Snow water equivalent

The average SWE for the years 2012–2017 varied from  $288.7 \pm 106.8$  to  $758.4 \pm 261$  mm over the Vestre Broggerbeen, while for the Feiringbeen, it

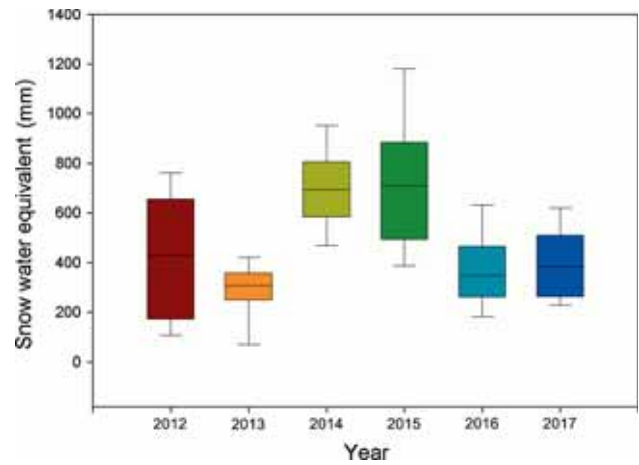


Figure 6. Temporal pattern of SWE over the Vestre Broggerbeen glacier for the year 2012–2017.

was  $381.9 \pm 187$  mm in the year 2016 (figures 6 and 4c). In Vestre Broggerbeen, the SWE over the ablation zone for the years 2012, 2013, 2014, 2015 and 2016 was  $400.6 \pm 220$ ,  $275.3 \pm 109$ ,  $630.8 \pm 166$ ,  $579.4 \pm 131$  and  $318.5 \pm 112$  mm, respectively. However, over the accumulation zone for the same years, it was  $754.4 \pm 78.8$ ,  $365.8 \pm 21$ ,  $821 \pm 159$ ,  $917.4 \pm 203$  and  $645.1 \pm 143$  mm, respectively. In the Feiringbeen glacier, the SWE was observed and showed  $649 \pm 119$  mm for the higher zone (>600 m.a.s.l.),  $373 \pm 82$  mm for the middle zone (400–600 m.a.s.l.) while  $139 \pm 67$  mm was observed for the lower zone (<400 m.a.s.l.).

### 3.4 Spatial pattern of snowpack characteristics

The pattern of spatial characteristics is shown in figure 7, in which the Vestre Broggerbeen glacier has a 55% area with a flat profile curvature and 60% area with a flat plan curvature. In the profile curvature, 31% area is concave (<0) and 14% area is convex (>0); however, in the plan curvature, 14.5% area is concave (<0) and 25.7% area is convex (>0). Both curvatures (plan and profile) give an understanding of flow across the surface. The profile curvature affects the acceleration and deceleration of flow and the plan curvature influences convergence and divergence of flow. Vestre Broggerbeen is NE facing and, the major area of glacier (56%) is within 0–90 (NE) flowing and the least area (2%) is within 180–270 (SW) flow, However, only 24% and 20% area is within the 270–359 (SW) and 180–270 (SW) flows, respectively. In the slope categories, maximum glaciers' area (42%) is in 5–10° class, followed by 0–5° (23%), 5–10° (15%), >20° (13%) and 15–20° (7%).

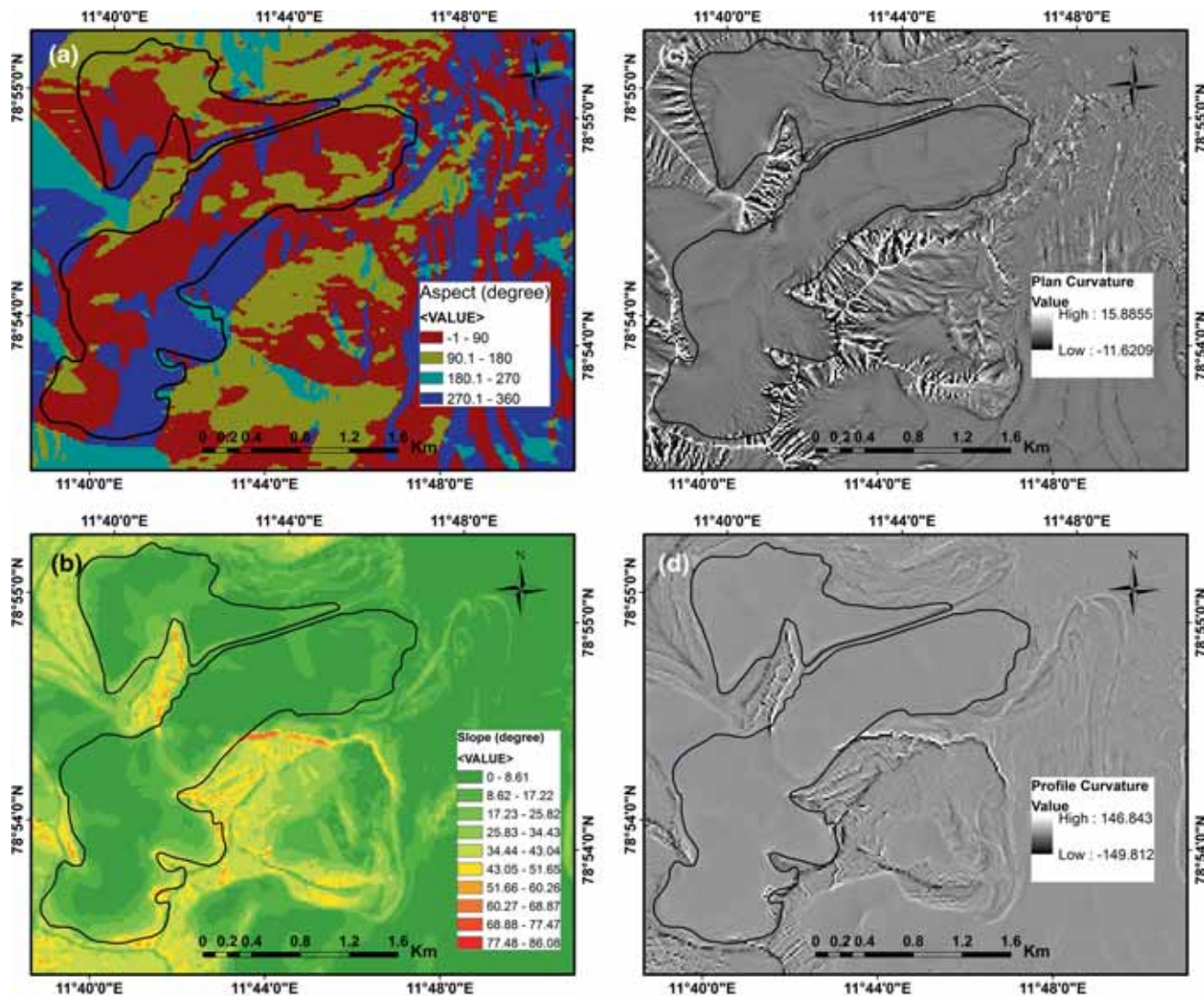


Figure 7. Spatial characteristics of the Vestre Broggerbreen glacier: (a) aspect, (b) slope, (c) plan curvature and (d) profile curvature.

As per the spatial pattern of curvature, aspect and slope, the spatial characteristics of the surveyed point's locations have been extracted and summarised in table 2. The distribution of the average snowpack characteristics (snow density, snow depth and SWE) is presented in table 3. Average snow density for all the spatial characteristics except aspect (180–270°) and slope class ( $>20^\circ$ ) were ranging from 0.36 to 0.38 g/cm<sup>3</sup>, while for other classes (aspect (180–270°) and slope class ( $>20^\circ$ )) was low due to the less number of surveyed points. The average snow depth (121.8 cm) and SWE (459.1 mm) were high in the convex curvature ( $<0$ ) compared to concave curvature (115.7 cm and 433.4 mm). The glacier zone within the north and the west zone (NW) was with the higher average snow depth (142.3 cm) and SWE (536.9 mm) while the zone within the SE direction

was lower average snow depth (98.9 cm) and SWE (377.1 mm). The zone with direction SW was not considered, due to less number of surveyed points. In the slope class, the high average snow depth (127.8 cm) and SWE (453.3 mm) was observed in the zone between  $10^\circ$  and  $15^\circ$ , while low average snow depth (117.6 cm) was in the zone with  $0\text{--}5^\circ$  slope and low SWE (443.3 mm) was observed in the zone with  $15\text{--}20^\circ$ .

#### 4. Discussion

The distribution pattern of snow depth over Vestre Broggerbreen during 2012–2017 revealed the lowest average snow depth ( $77.5 \pm 27.3$  cm) in the year 2013 and the highest average snow depth ( $181.6 \pm 43.2$  cm) in 2014. A decreasing trend was

Table 3. *The variation of snow density, snow depth and SWE among different spatial characteristics.*

	Class	<i>N</i>	Average snow density	Average snow depth	SWE
Curvature	<0	117	0.38	121.8	459.1
	>0	159	0.38	115.7	433.4
Aspect (deg)	0–90 (NS)	180	0.38	118.4	442.9
	90–180 (SE)	53	0.38	98.9	377.1
	180–270 (SW)	1	0.32	116.7	369.8
	270–360 (NW)	42	0.37	142.3	536.9
Slope (deg)	0–5	112	0.38	117.6	444.4
	5–10	138	0.37	120.0	448.4
	10–15	20	0.36	127.8	453.3
	15–20	22	0.36	123.1	443.3
	>20	2	0.32	119.2	377.8

observed in snow depth over Vestre Broggerbreen. Such a decreasing trend of snow accumulation in this region could be due to the reduced snow precipitation or increased liquid precipitation. Most winter precipitation is connected with an inflow of relatively warm air masses from the Norwegian Sea (Forland and Hanssen-bauer 2000). Similarly, decreasing snow cover has been reported at Vestfonna and De Geerfonna ice caps (Möller *et al.* 2011). López-Moreno *et al.* (2016) reported the decreased solid precipitation over the Ny-Ålesund region by analysing the available data for the period 1996–2013 and Van Pelt *et al.* (2016) showed increasing liquid precipitation over the Svalbard region. There was no linear trend of snow depth observed over the glacier surface. Drifting of snow may be one of the controlling factors for snow distribution over glacier surface including catchment; however, the velocity of wind and topography of individual glacier may limit this factor. Sauter *et al.* (2013) have reported the role of wind in the inhomogeneous distribution of snow over the glacier especially during spring. The average wind speed for the winter time varies from 2 to 3.5 m/s (figure 8). The data revealed that most of the time wind was blowing from the SE to the NW, that is, katabatic wind followed by ESE to WNW during the studied period. Since the drifting and blowing occur in highly elevated regions, snow drift may not have a significant role in valley glaciers closed to the Ny-Ålesund region except two–three limited regions over the glacier such as the medial moraine, cliff, etc.

In the Ny-Ålesund region, snow cover generally appears in the second half of September and remains until the beginning of July. Increased climate variability over the Arctic region seems to

have influenced the snow cover seasons which have affected snow accumulation in autumn and winter (Van Pelt *et al.* 2016). The high difference in the snow thickness over the ablation and accumulation zone could be due to the effect of topography and wind re-deposition. Wind drift is a major factor influencing the snow precipitation in this region (Forland and Hanssen-bauer 2000). A similar impact has been reported from the field observations in the Hansbreen glacier by Laska *et al.* (2016). Generally, there is no clear trend that reflects the snow depth change. Apparently, different directions of snow thickness change in a particular glacier played a major role as a combined influence of regional air circulation condition, local precipitation pattern and topo-climatic conditions (Grabiec *et al.* 2011). Snow accumulation increases with elevation. The upper regions of glaciers have a high thickness of snow accumulation as compared to the lower part due to less snow drifting, low melting and increasing number of snowfall events. There was a difference in the snow distribution over the Vestre Broggerbreen and Feiringbreen for the year 2016. The average snow depth was comparatively higher in the Feiringbreen, while the snow depth gradient was similar in both the glaciers. The difference in the distribution may be due to the difference in the altitudinal range of both the glaciers.

The snowpack density varies from 0.26 and 0.50 g/cm<sup>3</sup> over the entire glacier. The density of the snowpack was found to increase from the surface to the ice snow interaction zone. Möller *et al.* (2011) have also reported higher density with increasing snow depth from the top to the bottom in the Vestfonna and De Geerfonna ice caps. The bulk density tends to increase with snowpack

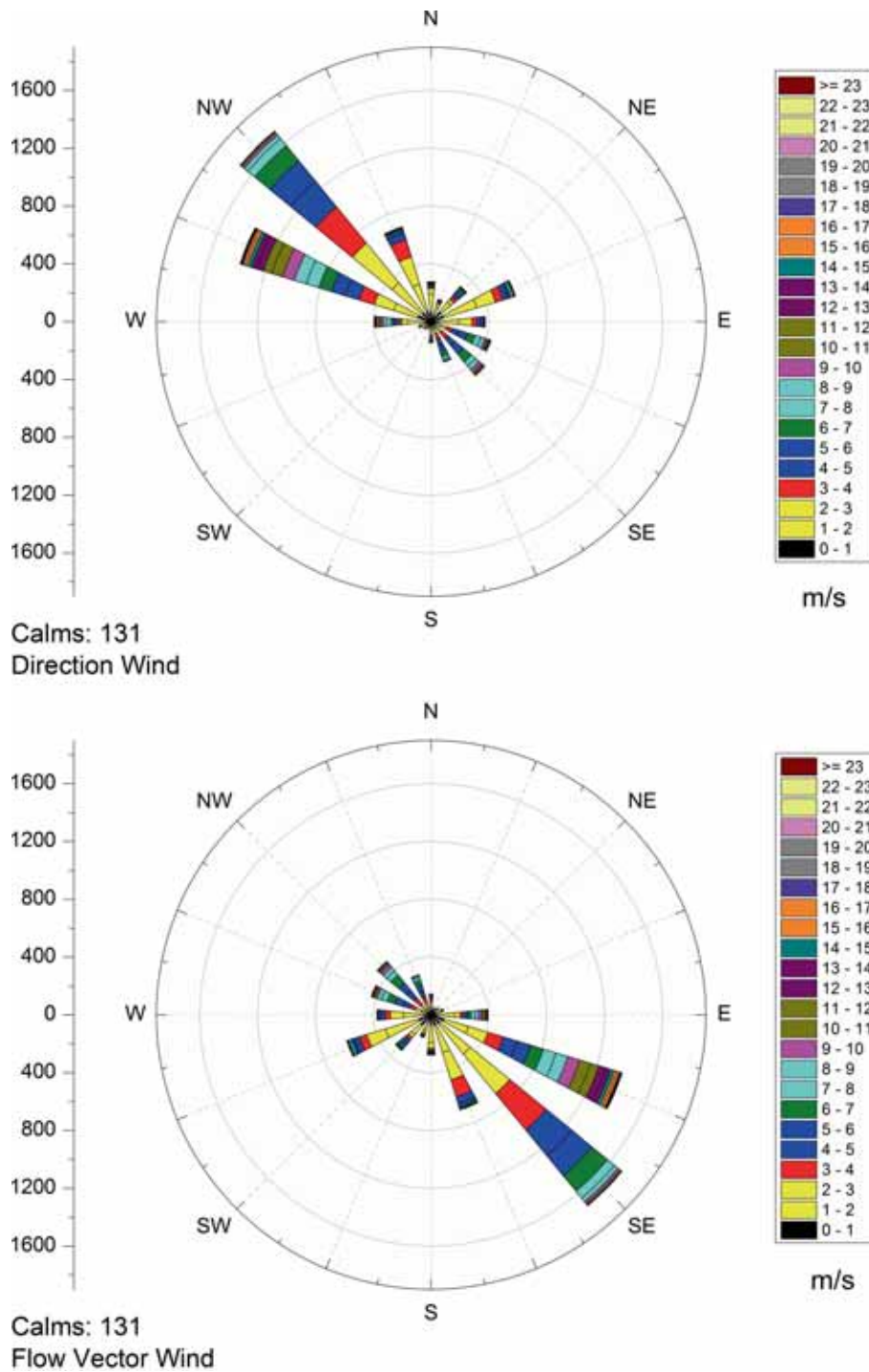


Figure 8. Wind pattern during the studied period in Ny-Ålesund, Svalbard.

thickness, because of the stronger compaction due to the increasing pressure of overlying snow. A study by Boike *et al.* (2003) in Ny-Ålesund reported densities to range between 0.35 and 0.40 g/cm<sup>3</sup>, for April 2000, and López-Moreno *et al.* (2016) has reported 0.38 ± 0.05 g/cm<sup>3</sup> on Vestfonna. Sturm *et al.* (2010) also reported a symmetrical distribution of mean density over three countries and two

continents. Apparently, compaction by wind drift seems to be the main reason. Wind drift comprises the only frequent agent that is able to assure continuous rounding on snow grains and thus densification of the snow cover. The wind deposited snow is usually characterised by a higher density than the undisturbed ones, where the grain size is smaller. Therefore, the snowpack is more compact

Table 4. Correlation matrix between snow depth, snow density, SWE and selected spatial variables.

	Snow density	Snow depth	SWE	Aspect	Curvature	Slope	Elevation
Snow density	1.00						
Snow depth	-0.05	1.00					
SWE	0.19	0.97	1.00				
Aspect	0.00	0.12	0.12	1.00			
Curvature	-0.05	-0.15	-0.16	0.06	1.00		
Slope	-0.20	0.04	-0.01	-0.04	-0.15	1.00	
Elevation	-0.24	0.65	0.57	0.14	-0.17	0.13	1.00

due to the rounding of the snow crystal during wind drift transport. The results showed the increased snow thickness has a higher influence on the snowpack density compared to the altitudinal pattern.

The statistical tests revealed a high significant correlation between the snow depth and SWE ( $R^2 = 0.97$  ( $n = 276$ ,  $p = <0.05$ )), compared to snow depth and elevation ( $R^2 = 0.65$ ), and SWE and elevation ( $R^2 = 0.57$ ) (table 4). Even though the general distribution of snowpack characteristics (snow density, snow depth and SWE) were high in the concave curvature, the zone within  $270\text{--}360^\circ$  (NW) and slope off between  $10^\circ$  and  $15^\circ$ , the statistical results showed no control of aspect, curvature and elevation over the snowpack distribution during the studied period.

The analysis indicated a highly significant correlation between snow depth and SWE compared to the altitude versus snow depth and altitude versus SWE across the Vestre Broggerbreen and Feiringbreen glaciers (figure 9). This clearly suggests the spatial control of snow depth over SWE compared to altitude. Möller *et al.* (2011) demonstrated the role of elevation for SWE spatial variability over the Ny-Ålesund region where the snow depth and altitude were the dominant factors in determining the spatial distribution of SWE across the Vestre Broggerbreen and Feiringbreen glaciers. López-Moreno *et al.* (2016) measured the SWE in the lower region (Bayeleva Station) of the Vestre Broggerbreen and found that for the spring season, the SWE varied from 190 to 230 mm. In the present study, there was no trend in the SWE for the studied period, and also showed an insignificant correlation ( $R = 0.3$ ;  $n = 6$ ) with the annual precipitation.

We compared the SWE pattern with the October–March precipitation and temperature data sets (figure 10) and obtained similar results. The correlation coefficient between SWE and precipitation

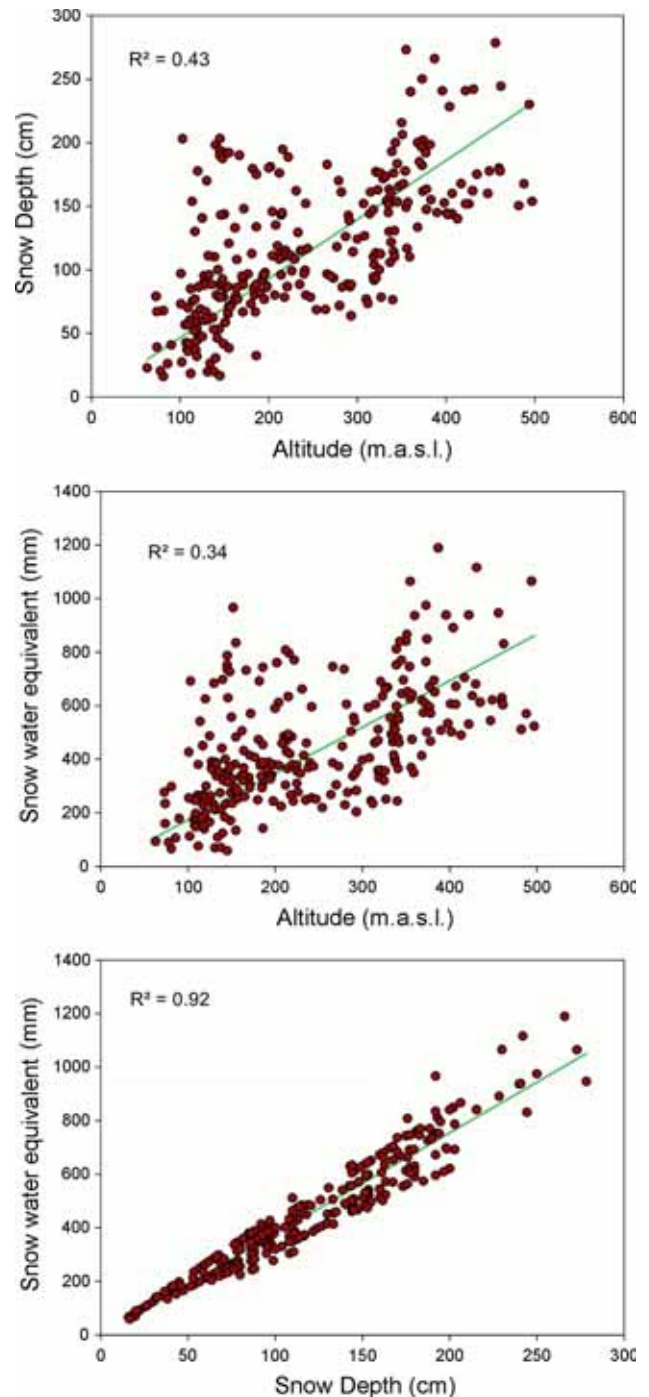


Figure 9. The spatial trend of SWE with snow depth over the selected glaciers of the Svalbard region for the studied period.

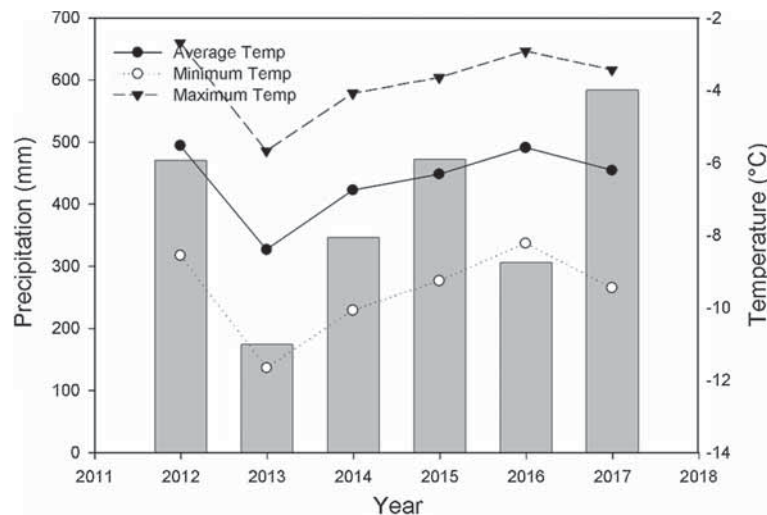


Figure 10. Early snow season (October–March) precipitation, mean, minimum and maximum temperature pattern for the period 2012–2017.

was  $R = -0.3$ ;  $n = 6$  for the whole period (October–March for 2012–2017). For the year 2013, precipitation was low and the SWE was also low. However, for the years 2014 and 2015, the precipitation was comparatively less (346 and 472 mm, respectively), but observed highest SWE (697 and 758 mm, respectively). We compared the data excluding the years 2013 and 2014. The results showed a significant correlation ( $R = -0.85$ ;  $n = 4$ ) with October–March precipitation. However, the correlation was negative, indicating that high precipitation leads to lower SWE. If the precipitation is snow, the relationship is expected to be positive. López-Moreno *et al.* (2016) reveal the influence of liquid precipitation and SWE, by decreasing the SWE in Ny-Ålesund. Although the present study was based on the observations for the limited period 2012–2017, previous studies also reported similar results from the decadal climate data analysis (Forland and Hanssen-bauer 2000; López-Moreno *et al.* 2016), implying the influence of liquid precipitation on SWE. If the atmospheric temperature is also high during precipitation, there could be chances of increased liquid precipitation.

To examine this, we have analysed precipitation and temperature data sets from Ny-Ålesund. High precipitation was recorded under high average temperature conditions except for the year 2016 (figure 11). The monthly average temperature (mean, maximum and minimum) was below  $0^{\circ}\text{C}$ , but the daily average temperature was higher than  $0^{\circ}\text{C}$  for several days for the period 2012–2017. The correlation analysis for the precipitation and mean temperature was positive ( $R = 0.87$ ,  $n = 5$ ,

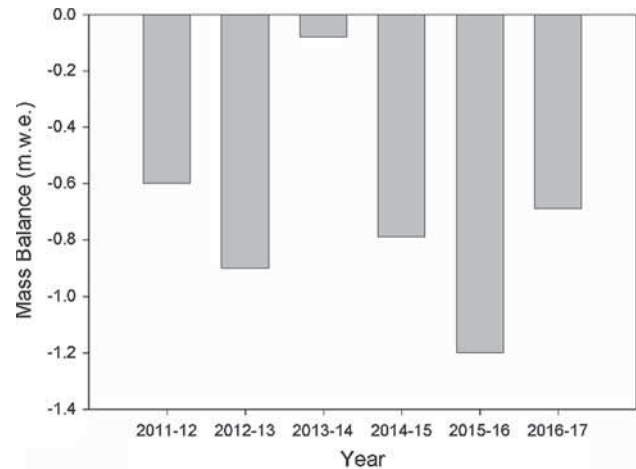


Figure 11. SMB of the Vestre Broggerbeen glacier for the period 2012–2017.

$p < 0.05$ ) except for the year 2016 (figure 11). In Ny-Ålesund, temperature and precipitation have been increasingly controlled by the southerly winds (Maturilli *et al.* 2013), particularly in winter. As the southerly winds are warm and moist, enhanced precipitation might have recorded, in the liquid form.

The annual SMB of the Vestre Broggerbeen glacier since 2012 is given in figure 11. The overall glacier-wide net annual SMB of the Vestre Broggerbeen glacier was  $-0.59 \pm 0.12$ ,  $-0.94 \pm 0.19$ ,  $-0.08 \pm 0.02$ ,  $-0.79 \pm 0.16$ ,  $-1.22 \pm 0.24$  and  $-0.69 \pm 0.14$  m.w.e. for years 2012–2013, 2013–2014, 2014–2015, 2015–2016 and 2016–2017, respectively. Available data reflect that this glacier has experienced negative annual balance since 2012 and lost a cumulative mass of  $3.28 \times 10^3$  ton

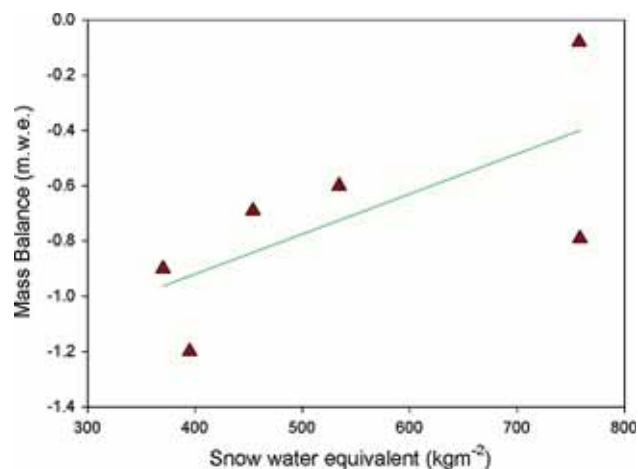


Figure 12. Relationship between the SWE and SMB of Vestre Broggerbreen glacier for the period 2012–2017.

(4.31 m.w.e.) of glacier ice during the past 6 years (figure 11). The study revealed that SWE is one of the highly significant factors controlling the mass budget of the studied glaciers in Ny-Ålesund (figure 12). Since winter snow accumulation over the glacier surface is one of the common factors for estimating SWE and winter/spring balance of the corresponding glacier, SWE has a significant impact on the annual mass budget of the respective glacier. While the annual mass balance is governed by many other factors such as temperature, humidity, solar radiation and wind conditions, the relation is not linear. Statistical analysis showed a significant positive correlation ( $R = 0.72$ ,  $n = 5$ ,  $p = <0.05$ ) between the SWE and net annual SMB for the period 2012–2017. However, both (SWE and net SMB) have an inverse relation with precipitation caused by the increasing ratio of liquid precipitation during 2012–2017. The increasing ratio of liquid precipitation affects accumulation by refreezing the layers and providing additional energy (heat) to the snowpack during refreezing processes that reduce the cold content of the snowpack. Although the snow cover over the glacier protects the glacier from the incoming solar radiation, the presence of the refreezing layers over the glacier leads the incoming solar radiation to get trapped due to the reduced albedo of the refreezing mass, which enhances the ablation processes over the glacier surface. Although the precipitation increased during the last 5 years, a significant increase in liquid precipitation has reduced the SWE and increased the total mass wastage of the Vestre Broggerbreen and Feiringbreen glaciers in the Ny-Ålesund region.

## 5. Conclusions

The SWE is one of the crucial factors controlling the mass budget of glaciers in the Ny-Ålesund region. The spatial and temporal variability of the SWE was studied using the field data during 2012–2017. This study revealed a significant reduction in snow depth across the glacier during the past 6 years, even though the average mean density of the snowpack is almost similar throughout the studied period. The observed data showed a significant reduction in the SWE during the last 4 years from 2014 to 2017 without any linear trend. Since there is no significant change observed in snow density, the reduction in SWE ( $R^2 = 0.97$  ( $n = 276$ ,  $p = <0.05$ )) is due to the decrease in snow depth across the glacier in the Ny-Ålesund region. The distribution of snow over the glaciers is mostly controlled by the precipitation in this region, followed by altitude and wind drift. The spatial analysis of this glacier has ruled out any significant role of aspect and curvature over the snowpack. The study revealed that the SWE across the glacier has reduced significantly due to the increase in liquid precipitation during winter that is governed by the southerly winds over the Ny-Ålesund region which has a crucial impact over the net annual SMB of the glaciers in this region. Vestre Broggerbreen glacier lost more than 4 m.w.e. ice throughout the glacier since 2012. Further high-resolution precipitation and wind data could quantify the control of liquid precipitation, wind over the SWE.

## Acknowledgements

This work is part of the project ‘Cryosphere and Climate’ funded by the Ministry of Earth Sciences, India. We thank the director, ESSO-National Centre for Polar and Ocean Research, Goa, for the continued support. We also acknowledge the logistic support of the Arctic division at NCAOR. The US Geological Survey (USGS) is acknowledged for the Landsat images and the Norwegian Polar Institute, for the digital elevation model. The Norwegian Meteorological Institute is also acknowledged for providing weather datasets. We are also thankful to the two anonymous reviewers, for their suggestions and comments towards the improvement of the manuscript. This is NCPOR contribution no. J-8/2019-20.

## References

- Arnold N S, Rees W G, Hodson A J and Kohler J 2006 Topographic controls on the surface energy balance of an Arctic valley glacier; *J. Geophys. Res.: Earth Surf.* **111**(F2) 1–15 (F02011), <https://doi.org/10.1029/2005jf000426>.
- Bavera D, Bavay M, Jonas T, Lehning M and Michele De C 2014 A comparison between two statistical and a physically-based model in snow water equivalent mapping; *Adv. Water. Resour.* **63** 167–178, <https://doi.org/10.1016/j.advwatres.2013.11.011>.
- Bocchiola D and Rosso R 2007 The distribution of daily snow water equivalent in the central Italian Alps; *Adv. Water. Resour.* **30**(1) 135–147, <https://doi.org/10.1016/j.advwatres.2006.03.002>.
- Boike J, Roth K and Ippisch O 2003 Seasonal snow cover on frozen ground: Energy balance calculations of a permafrost site near Ny-Ålesund, Spitsbergen; *J. Geophys. Res. Atmos.* **108**(D1) 8163, <https://doi.org/10.1029/2001JD000939>.
- Bruland O and Sand K 2001 Snow distribution at a high Arctic site at Svalbard; *Nord. Hydrol.* **32**(1) 1–12.
- Bruland O, Liston G E, Vonk J, Sand K and Killingtveit Å 2004 Modelling the snow distribution at two high Arctic sites at Svalbard, Norway, and at an alpine site in central Norway; *Nord. Hydrol.* **35**(2001) 191–208.
- Callaghan T V, Johansson M, Brown R D, Groisman P Y, Labba N, Radionov V, Barry R G, Bulygina O N, Essery R H L, Frolov D M, Golubev V N, Grenfell T C, Petrushina M N, Razuvaev V N, Robinson D A, Romanov P, Shindell D, Shmakin A B, Sokratov S A, Warren S and Yang D 2011 The changing face of Arctic snow cover: A synthesis of observed and projected changes; *Ambio* **40**(Suppl. 1) 17–31, <https://doi.org/10.1007/s13280-011-0212-y>.
- Clark M P, Hendriks J, Slater A G, Kavetski D, Anderson B, Cullen N J, Kerr T, Hreinsson E O and Woods R A 2011 Representing spatial variability of snow water equivalent in hydrologic and land-surface models: A review; *Water Resour. Res.* **47**(7) 1–23, <https://doi.org/10.1029/2011WR010745>.
- Clow D W, Nanus L, Verdin K L and Schmidt J 2012 Evaluation of SNODAS snow depth and snow water equivalent estimates for the Colorado Rocky Mountains, USA; *Hydrol. Process.* **26**(17) 2583–2591, <https://doi.org/10.1002/hyp.9385>.
- Cogley J G, Hock R and Rasmussen L A *et al.* 2011 Glossary of glacier mass balance and related terms; IHP-VII Technical Documents in Hydrology No.86, IACS Contribution No. 2, Paris, UNESCO-IHP, p. 114.
- Cornwell E, Molotch N P and McPhee J 2016 Spatio-temporal variability of snow water equivalent in the extra-tropical Andes Cordillera from distributed energy balance modeling and remotely sensed snow cover; *Hydrol. Earth Syst. Sci.* **20**(1) 411–430, <https://doi.org/10.5194/hess-20-411-2016>.
- Derksen C and Brown R 2012 Spring snow cover extent reductions in the 2008–2012 period exceeding climate model projections; *Geophys. Res. Lett.* **39**(19), <https://doi.org/10.1029/2012GL053387>.
- Eckerstorfer M and Christiansen H H 2011 Topographical and meteorological control on snow avalanching in the Longyearbyen area, central Svalbard 2006–2009; *Geomorphology* **134**(3–4) 186–196, <https://doi.org/10.1016/j.geomorph.2011.07.001>.
- Egli L, Jonas T and Meister R 2009 Comparison of different automatic methods for estimating snow water equivalent; *Cold. Reg. Sci. Technol.* **57**(2–3) 107–115, <https://doi.org/10.1016/j.coldregions.2009.02.008>.
- Forland E J and Hanssen-bauer I 2000 Increased precipitation in the Norwegian Arctic: True or false?; *Clim. Change* **46** 485–509, <https://doi.org/10.1023/A:1005613304674>.
- Foster J L, Sun C and Walker J P *et al.* 2005 Quantifying the uncertainty in passive microwave snow water equivalent observations; *Remote Sens. Env.* **94**(2) 187–203, <https://doi.org/10.1016/j.rse.2004.09.012>.
- Godio A and Rege R B 2016 Analysis of georadar data to estimate the snow depth distribution; *J. Appl. Geophys.* **129** 92–100, <https://doi.org/10.1016/j.jappgeo.2016.03.036>.
- Grabiec M, Puczko D, Budzik T and Gajek G 2011 Snow distribution patterns on Svalbard glaciers derived from radio-echo soundings; *Pol. Polar Res.* **32**(4) 393–421, <https://doi.org/10.2478/v10183-011-0026-4>.
- Hagen J O, Kohler J, Melvold K and Winther J 2003 Glaciers in Svalbard: Mass balance, runoff and freshwater flux; *Polar Res.* **22**(2) 145–159, <https://doi.org/10.1111/j.1751-8369.2003.tb00104.x>.
- Hallinger M, Manthey M and Wilmking M 2010 Establishing a missing link: Warm summers and winter snow cover promote shrub expansion into alpine tundra in Scandinavia; *New Phytol.* **186**(4) 890–899, <https://doi.org/10.1111/j.1469-8137.2010.03223.x>.
- Holbrook W S, Miller S N and Provart M A 2016 Estimating snow water equivalent over long mountain transects using snowmobile-mounted ground-penetrating radar; *Geophysics* **81**(1) WA183–WA193, <https://doi.org/10.1190/geo2015-0121.1>.
- Jonas T, Marty C and Magnusson J 2009 Estimating the snow water equivalent from snow depth measurements in the Swiss Alps; *J. Hydro. (Amst)* **378**(1–2) 161–167, <https://doi.org/10.1016/j.jhydrol.2009.09.021>.
- Kerner F, Obleitner F, Krismer T, Kohler J and Greuell W 2013 A decade of energy and mass balance investigations on the glacier Kongsvegen, Svalbard; *J. Geophys. Res. Atmos.* **118**(10) 3986–4000, <https://doi.org/10.1029/2012jd018342>.
- Laska M, Luks B and Budzik T 2016 Influence of snowpack internal structure on snow metamorphism and melting intensity on Hansbreen, Svalbard; *Pol. Polar Res.* **37** 193–218, <https://doi.org/10.1515/popore-2016-0012>.
- Liston G E and Sturm M 2002 Winter precipitation patterns in Arctic Alaska determined from a blowing-snow model and snow-depth observations; *J. Hydrometeorol.* **3**(6) 646–659, [https://doi.org/10.1175/15257541\(2002\)003%3c0646:WPPIAA%3e2.0.CO;2](https://doi.org/10.1175/15257541(2002)003%3c0646:WPPIAA%3e2.0.CO;2).
- López-Moreno J I, Fassnacht S R, Heath J T, Musselman K N, Revuelto J, Latron J, Tejeda E M and Jonase T 2013 Small scale spatial variability of snow density and depth over complex alpine terrain: Implications for estimating snow water equivalent; *Adv. Water. Resour.* **55** 40–52, <https://doi.org/10.1016/j.advwatres.2012.08.010>.
- López-Moreno J I, Boike J, Sanchez-Lorenzo A and Pomeroy J W 2016 Impact of climate warming on snow processes in Ny-Ålesund, a polar maritime site at Svalbard; *Glob. Planet. Change* **146** 10–21, <https://doi.org/10.1016/j.gloplacha.2016.09.006>.
- Maturilli M, Herber A and König-Langlo G 2013 Climatology and time series of surface meteorology in Ny-Ålesund,

- Svalbard; *Earth Syst. Sci. Data* **5**(1) 155–163, <https://doi.org/10.5194/essd-5-155-2013>.
- Möller M, Möller R, Beaudon E, Mattila O P, Finkelnburg R, Braun M, Grabiec M, Jonsell U, Luks B, Puczko D, Scherer D and Schneider C 2011 Snowpack characteristics of Vestfonna and de Geerfonna (Nordaustlandet, Svalbard) – A spatiotemporal analysis based on multiyear snow-pit data; *Geogr. Ann. A* **93**(4) 273–285, <https://doi.org/10.1111/j.1468-0459.2011.00440.x>.
- Pälli A, Kohler J C, Isaksson E and Moore J C 2002 Spatial and temporal variability of snow accumulation using ground-penetrating radar and ice cores on a Svalbard glacier; *J. Glaciol.* **48**(162) 417–424, <https://doi.org/10.3189/172756502781831205>.
- Paterson W S B 1994 *The physics of glaciers* (3rd edn); Elsevier, Oxford, pp. 26–52, ISBN 9780080379449, <https://doi.org/10.1016/C2009-0-14802-X>.
- Rice R, Bales R C, Painter T H and Dozier J 2011 Snow water equivalent along elevation gradients in the Merced and Tuolumne river basins of the Sierra Nevada; *Water Resour. Res.* **47**(8) 1–11, <https://doi.org/10.1029/2010WR009278>.
- Sauter T, Möller M, Finkelnburg R, Grabiec M, Scherer D and Schneider C 2013 Snowdrift modelling for the Vestfonna ice cap, north-eastern Svalbard; *Cryosphere* **7** 1287–1301, <https://doi.org/10.5194/tc-7-1287-2013>.
- Serreze M C, Barrett A P, Stroeve J C, Kindig D N and Holland M M 2009 The emergence of surface-based Arctic amplification; *Cryosphere* **3** 11–19, <https://doi.org/10.5194/tcd-2-601-2008>.
- Sihvola A and Tiuri M 1986 Snow fork for field determination of the density and wetness profiles of a snow pack; *IEEE Trans. Geosci. Remote Sens.* **GE-24**(5) 717–721, <https://doi.org/10.1109/TGRS.1986.289619>.
- Skaugen T 2007 Modelling the spatial variability of snow water equivalent at the catchment scale; *Hydrol. Earth Syst. Sci.* **11**(5) 1543–1550, <https://doi.org/10.5194/hess-11-1543-2007>.
- Sturm M, Taras B, Liston G E, Derksen C, Jonas T and Lea J 2010 Estimating snow water equivalent using snow depth data and climate classes; *J. Hydrometeorol* **11**(6) 1380–1394, <https://doi.org/10.1175/2010JHM1202.1>.
- Van Pelt W J J, Kohler J, Liston G E, Hagen J O, Luks B, Reijmer C H and Pohjola V A 2016 Multidecadal climate and seasonal snow conditions in Svalbard; *J. Geophys. Res. Earth. Surf.* **121**(11) 2100–2117, <https://doi.org/10.1002/2016JF003999>.
- Wagnon P, Linda A, Arnaud Y, Kumar R, Sharma P, Vincent C, Pottakkal J G, Berthier E, Ramanathan A L, Hasnain S I and Chevallier P 2007 Four years of mass balance on Chhota Shigri glacier, Himachal Pradesh, India: A new benchmark glacier in the western Himalaya; *J. Glaciol.* **53**(183) 603–611, <https://doi.org/10.3189/002214307784409306>.
- Zemp M, Thibert E, Huss M, Stumm D, Denby C R, Nuth C, Nussbaumer S U, Moholdt G, Mercer A, Mayer C, Joerg P C, Jansson P, Hynek B, Fischer A, Escher-Vetter H, Elvehøy H and Andreassen L M 2013 Reanalysing glacier mass balance measurement series; *Cryosphere* **7** 1227–1245, <https://doi.org/10.5194/tc-7-1227-2013>.

Corresponding editor: C GNANASEELAN